PhD Thesis

PhD Thesis

PhD Thesis

by Niclas Lars Rudolf Fiedler, M.Sc.
from Weilmünster

XX.XX.2028

Justus Liebig University Gießen
Institute of Experimental Physics II

First Examiner: Prof. Dr. Kai-Thomas Brinkmann
Second Examiner: Prof. Dr. Jens Sören Lange, AkR
Supervisor: Dr. Dzmitry Kazlou

Abstract

Zusammenfassung

Contents

Chapter 1

Detector Design and Construction

1.1 Introduction & Motivation

1.2 Detector Concept & Scintillator Selection

Two different scintillation-based detector-concepts were developed to measure the depth dose distribution of protons in real-time. Both detectors consist of 32 scintillator-layers read-out via **Si**licon **P**hoto**M**ultipliers (SiPMs) and two 16-channel CAEN digitizer that are linked together.

The first detector concept is, as the first prototype $PbWO_4$-based, [citemaster], but improves on the layer geometry by using sheets instead of bars whilst also reducing layer thickness. For this two crystal sizes were chosen with $30 \times 30 \times 3$ mm^3 and $30 \times 30 \times 2$ mm^3, which were provided and cut by Crytur, allowing full coverage of the 220 MeV proton range of ≈ 66 mm. The lateral sheet sizes with 30 mm were the largest providable, because the sheets were cut from a single ingot and the thicknesses are the smallest resonable due to $PbWO_4$ being very fragile. The 3 mm thick sheets are used in the front or shallow beam depths to provide more stopping power and the thinner 2 mm sheets are used in the Bragg-Peak region to give an optimal spatial resolution.

To further increase the spatial resolution in the Bragg-Peak region a second detector concept using plastic scintillators was developed. Plastic scintillators have a much lower density and thereby stopping power than $PbWO_4$, allowing the use of thicker scintillators whilst increasing the spatial resolution.

with a thicknes s of 4 mm allowing for a better spatial resolution. However, since the 32 available channels with 4 mm Ej-212 only cover $\approx$ 12.8 cm of the 30.4 cm proton range, a passive absorber has to be included to fully stopp the protons inside the detector. This 20 cm passive absorber consists of PMMA resulting in enough stopping power to stop the beam inside the detector. The passive absorber is placed between the first and second plastic scintillator such that the first works as a trigger channel which is used for the normalization in the analysis.

1.3 Readout

The scintillators of both designs are read out via SiPMs. Light yield measurements were conducted, to decide which SiPM types are suitable. With these the amount of incident photons can be estimated and compared with the number of pixel. From this, a balance can be struck between high resolution and a large enough dynamic range.

1.3.1 Light Yield Measurement

The measurements were conducted using the process described in Section **??** and the setup shown in Figure **??**. The PMT used is an R2059 from Hamamatsu (serial number BA3200) with a quantum efficiency of 23.16 % [1] (cf. Appendix **??**) at the luminescence peak of 420 nm of $PbWO_4$ [2] and EJ212.

1.3.1.1 Light Yield: $PbWO_4$

The $PbWO_4$ measurement were done in a flat and vertical position as shown in Figure **??**, where all non PMT-facing scintillator sides were enveloped in highly reflective PTFE foil in order to not lose any photons. Two additional measurements were performed, where one 3 mm- and 2 mm crystal were fully wrapped with an SiPM sized window cutout in the center of one side as shown in Figure **??**. The $PbWO_4$ crystals were mounted onto the PMT's optical window next to a ^{22}Na γ-source inside a climate chamber. The optical coupling was done using glycerol ($n = 1.4722$), as shown in Figure **??**. Glycerin was used as a substitute for the commonly used Baysilone® Fluid M optical grease ($n \approx 1.404$, $\eta = 300\,000\,\mathrm{mm^2/s}$ [3]), due to its less-adhesive characteristic. The Baysilone® Fluid M with its high adhesion might have lead to damaging the fragile crystals during removal. The refractive index of $PbWO_4$ and the SiO_2 glass window of the **P**hoto**M**ultiplier **T**ube (PMT) are $n_{\mathrm{PbWO_4}} \approx 2.3$ [2] and $n_{\mathrm{SiO_2}} \approx 1.459$ [4], respectively. Additionally to the climate chamber's light-tightness, the setup is enclosed in PTFE foil, ensuring perfect light tightness.

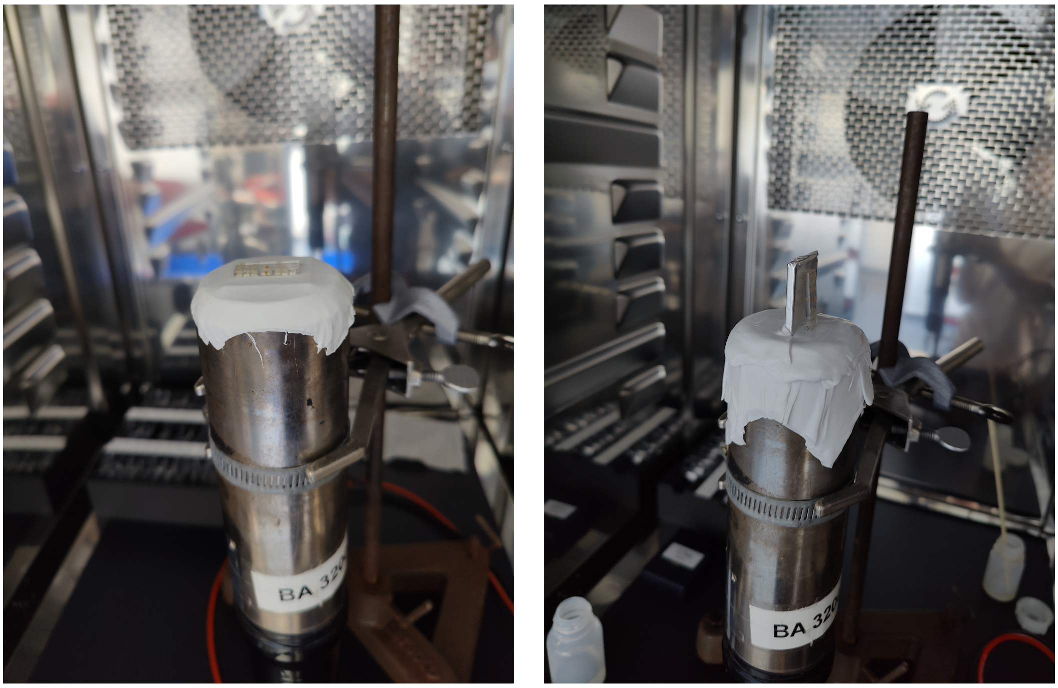

(a) Flat position. (b) Vertical position.

Figure 1.1: Measurement positions of the $PbWO_4$ scintillators on the PMT for the light yield measurements using a ^{22}Na source.

The measurements were conducted at 20 °C for 5 min after an acclimation time of 5 min each. The acclimation time was chosen small because the crystals were keept inside the climate chamber for 24 h before the measurements were startet, thereby only the short time frame inbetween measuements, where the chamber was opened, had to be accounted for. An exemplary light yield measurement of crystal number 0 in the flat position is shown in Figure 1.2. The measured light yield values of all crystals and their averages for the different setups are shown in Figure 1.3. The 3 mm thick crystals average approximately 164.73 ph/MeV and 129.44 ph/MeV in the flat and vertical positions, respectively. The 2 mm thick crystals average approximately 131.00 ph/MeV and 94.32 ph/MeV in the flat and vertical positions, respectively. With the SiPM-sized window cutout the light yield of a 3 mm and 2 mm crystal was (75.25 ± 33.09) ph/MeV and (59.70 ± 19.22) ph/MeV, respectively.

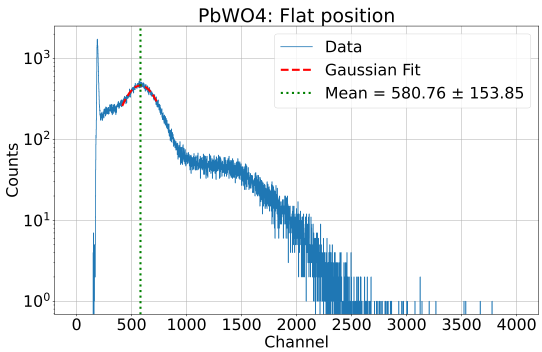

Figure 1.2: Example light yield measurement of the 3 mm thick $PbWO_4$-crystal number 0 in flat position on the PMT using a ^{22}Na source.

1.3.1.2 Light Yield: EJ-200

The light yield of a $50 \times 50 \times 10$ mm^3 EJ-200 sample was measured to estimate the amount of incident photons on an SiPM optically coupled to an EJ-212 scintillator, which has similar properties to EJ-200, to decide which SiPM type is needed for the readout.

The measurements were done in a flat and vertical position, with two source positions for the vertical setup, as shown in Figure 1.4. In the vertical position two wrappings for the scintillator were used. First the whole PMT facing side was left open and secondly only an SiPM-sized window cutout was left open. The scintillator was mounted onto the PMT's optical window inside a climate chamber and optically coupled using Baysilone® Fluid M optical grease [3]. The setups were fully enclosed in PTFE foil to ensure light-tightness. The source positions were on the side and on top of the scintillator. A ^{241}Am source was chosen due to the high light yield of EJ200 as ^{241}Am has a prominent low-energy gamma line at 59.6 eV.

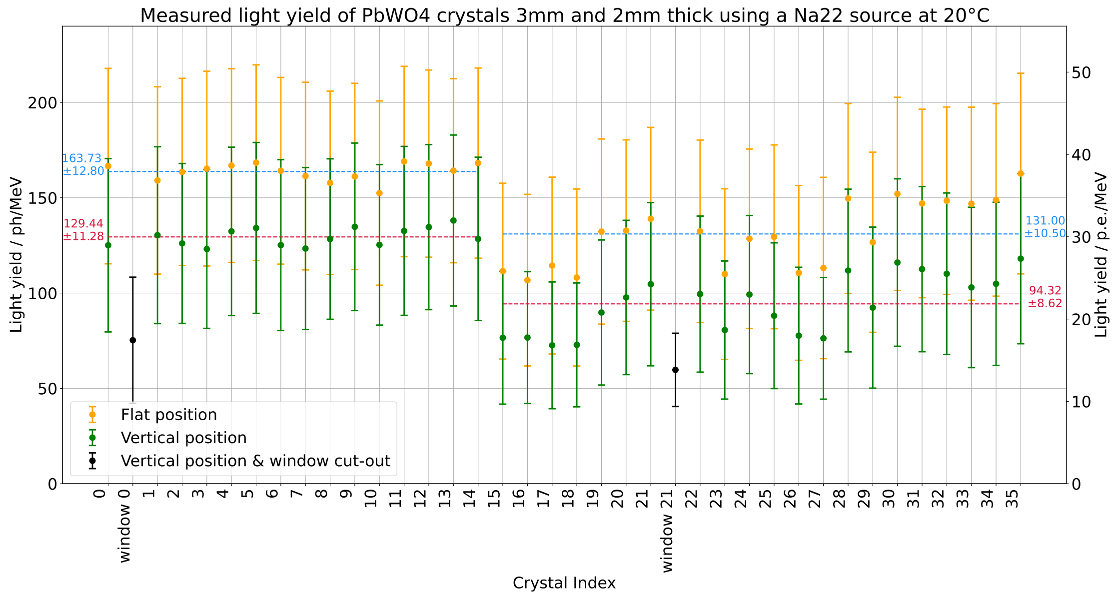

Figure 1.3: Light yield measurements of $PbWO_4$-crystals in flat and vertical positions including two window cut-out measuremetns using a ^{22}Na source.

The measurements were conducted at 20 °C for 20 min after an acclimation time of 24 h. The measurements and Gaussian fits of the 59.6 eV peak are shown in Figure 1.5.

The light yield results are shown in Table 1.1. The light yield for the flat position with is in good aggreement with the value provided by the manufacturer of 10 000 ph/MeV, taking into account aging-related degradation of the PMT (from 2012), which reduce the quantum efficiency. For both vertical positions, the light yield is only slightly affected by the source position. This is due to the high attenuation length of optical photons in the scintillator of 380 cm. When photons are collected from one side, approximately 30 % of the total light is lost and when using an SiPM-sized window cut-out the light yield is reduced by 70 %.

1.4 Photon Readout and SiPM Selection

An optimal SiPM-type for measuring the proton depth-dose distribution for the given scintillators needs to balance a high resolution with a high dynamic range to accurately measure the low energies in the shallow depths and the high energies in the Bragg-Peak

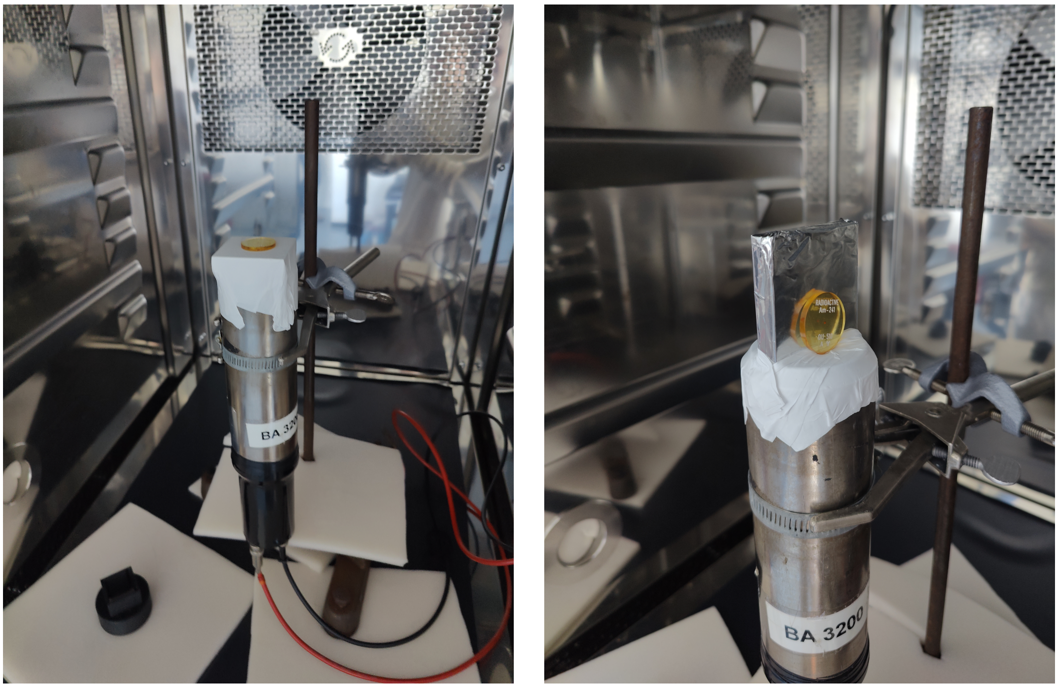

(a) Flat position. (b) Vertical position.

Figure 1.4: Measurement positions of the EJ-200 scintillator on the PMT for the light yield measurements using a ^{241}Am source.

region. To ensure a linear SiPM signal, the number of impinging photons needs to be less or equal to approximately 10 % of the number of pixels divided by the **P**hoto-**D**etection **E**fficiency (PDE).

1.4.1 SiPM for $PbWO_4$

The light yield measurements of the teflon-wrapped $PbWO_4$ crystals with an SiPM-sized window cutout resulted in (75.25 ± 33.09) ph/MeV and (59.70 ± 19.22) ph/MeV for the 3 mm and 2 mm thick crystal, respectively. The SiPM-type chosen, was the already available Broadcom AFBR-S4N44P014M, with an active area of 3.72×3.62 mm^2, a micro cell pitch of 40 µm, 8334 microcells and a maximum PDE of 63 % at 420 nm coinciding with the luminescence maximum of $PbWO_4$. The upper limit of the expected number of triggered pixels can be calculated using the highest simulated energy loss in the Bragg-Peak region, which is approximately 40 MeV, as shown in Figure **??**. Accounting for the

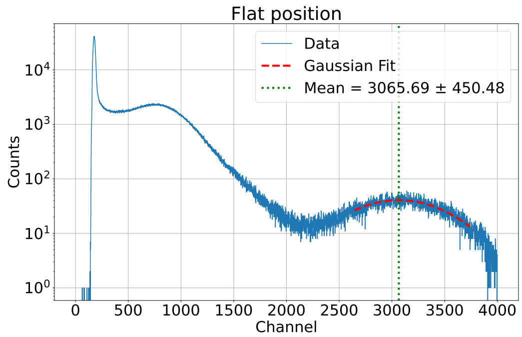

(a) Flat scintillator position.

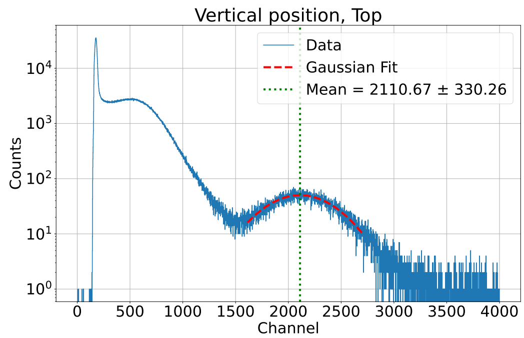

(b) Vertical position with open side and source on top.

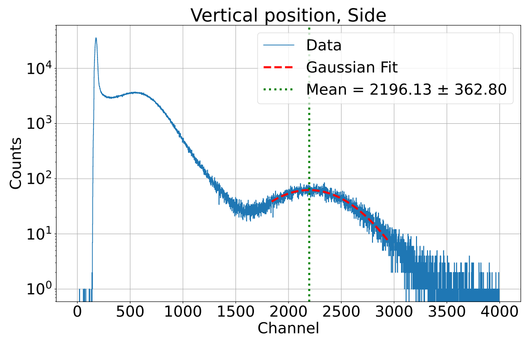

(c) Vertical position with open side and source on the side.

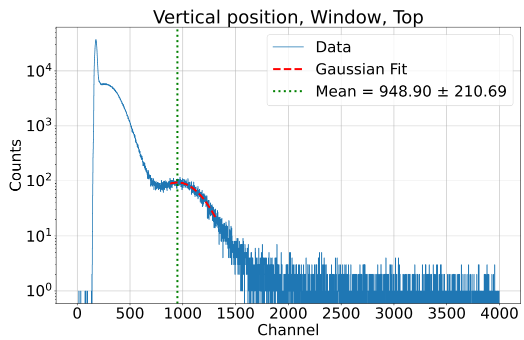

(d) Vertical position with SiPM-sized window cutout and source on top.

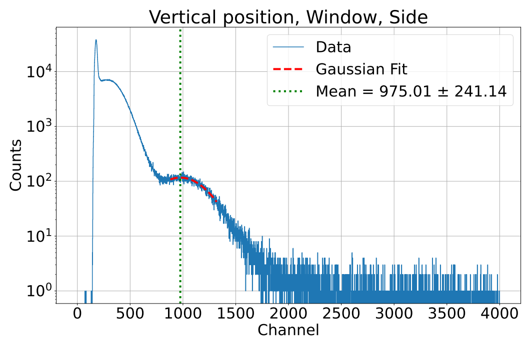

(e) Vertical position with SiPM-sized window cutout and source on the side.

Figure 1.5: Light yield measurements of the $50 \times 50 \times 10\mathrm{mm}^3$ EJ-200 scintillator sample. Shown are the measurements of the scintillator in a flat position with a completly open side (1.5a), in a vertical position with open side and the source on top (1.5b) and on the side (1.5c), and in a vertical position with an SiPM-sized window cutout with the source on top (1.5d) and on the side (1.5e).

Measurement	Peak position / ADC	Light yield / $\frac{\text{p.e.}}{\text{MeV}}$	Light yield / $\frac{\text{ph}}{\text{MeV}}$
Flat	3065.69 ± 450.48	1996.24 ± 301.74	8619.36 ± 1302.84
Vertical, Top	2110.67 ± 330.26	1356.56 ± 221.21	5857.33 ± 955.15
Vertical, Side	2196.13 ± 362.80	1413.80 ± 243.01	6104.49 ± 1049.26
Vertical, Window, Top	948.9 ± 210.69	578.39 ± 141.12	2497.35 ± 609.34
Vertical, Window, Side	975.01 ± 241.14	595.87 ± 161.52	2572.86 ± 697.41

Table 1.1: Light yield measurement results of the $50 \times 50 \times 10\text{mm}^3$ EJ-200 scintillator sample.

covered active area of the SiPM by the 2 mm thick crystal gives:

$$\frac{N(E)}{N(A)} = E \cdot \frac{L \cdot PDE}{N_0 \frac{A_{cov}}{A_{SiPM}}} \tag{1.1}$$

$$\frac{N(E_{max} = 40\,\text{MeV})}{N(A)} = 40\,\text{MeV} \cdot \frac{59.7\,\text{ph/MeV} \cdot 0.63\frac{1}{\text{ph}}}{N_0 \cdot \frac{2 \cdot 3.72\ \text{mm}^2}{3.62 \cdot 3.72\ \text{mm}^2}} \tag{1.2}$$

$$= 0.327 \tag{1.3}$$

1.4.2 SiPM for EJ-212

Since EJ-200 and EJ-212 are very similar the SiPM-type for the EJ-212 scintillators was chosen based on the measurements of EJ-200. The measured light yield for the teflon-wrapped EJ-200 scintillator with an SiPM-sized cut-out with a center positioned source is 2572.86 , as shown in Table 1.1. Due to the high light yield an SiPM, the Hamamatsu S14160-3010PS was chosen. This SiPM has an active area of $3 \times 3\text{mm}^2$, a micro cell pitch of 10 µm, 89984 microcells and a maximum PDE of 18 % at 460 nm, which is close to the luminescence maximum of EJ_{212} at 423 nm. The upper limit of the expected number of triggered pixels is again calculated using the highest simulated energy loss in the Bragg-Peak region, which is approximately 20 MeV, as shown in Figure **??**. Accounting for the fully covered active area of the SiPM this gives:

$$\frac{N(E)}{N_0} = E \cdot \frac{L \cdot PDE}{N_0} \tag{1.4}$$

$$\frac{N(E_{max} = 20\,\mathrm{MeV})}{N(A)} = 20\,\mathrm{MeV} \cdot \frac{2572.86\,\mathrm{ph/MeV} \cdot 0.18\,\frac{1}{\mathrm{ph}}}{N_0} \tag{1.5}$$

$$= 0.103 \tag{1.6}$$

1.5 Detector Assembly and Construction

1.6 Experimental Setup

1.7 Data Analysis

1.8 Results

1.9 Discussion

1.10 Outlook

Bibliography

[1] Hamamatsu Photonics. *R1828-01, R2059 Photomultiplier Tubes Datasheet*. Accessed: 2024-10-28. Hamamatsu Photonics K.K. 2019. URL: https://www.hamamatsu.com/content/dam/hamamatsu-photonics/sites/documents/99%5C_SALES%5C_LIBRARY/etd/R1828-01%5C_R2059%5C_TPMH1259E.pdf.

[2] *The CMS electromagnetic calorimeter project: Technical Design Report*. Technical design report. CMS. Geneva: CERN, 1997. URL: https://cds.cern.ch/record/349375.

[3] Bayer AG. *Baysilone® Fluids Brochure*. Accessed: 2024-10-30. 2020. URL: https://dcproducts.com.au/wp-content/uploads/2020/12/BayerBaysiloneFluidsBrochure.pdf.

[4] I. H. Malitson. "Interspecimen Comparison of the Refractive Index of Fused Silica". In: *J. Opt. Soc. Am.* 55 (Oct. 1965). DOI: 10.1364/JOSA.55.001205.

List of Figures

List of Tables

Selbstständigkeitserklärung

Hiermit versichere ich, die vorgelegte Thesis selbstständig und ohne unerlaubte fremde Hilfe und nur mit den Hilfen angefertigt zu haben, die ich in der Thesis angegeben habe. Alle Textstellen, die wörtlich oder sinngemäß aus veröffentlichten Schriften entnommen sind, und alle Angaben die auf mündlichen Auskünften beruhen, sind als solche kenntlich gemacht. Bei den von mir durchgeführten und in der Thesis erwähnten Untersuchungen habe ich die Grundsätze gute wissenschaftlicher Praxis, wie sie in der ‚Satzung der Justus-Liebig-Universität zur Sicherung guter wissenschaftlicher Praxis' niedergelegt sind, eingehalten. Entsprechend § 22 Abs. 2 der Allgemeinen Bestimmungen für modularisierte Studiengänge dulde ich eine Überprüfung der Thesis mittels Anti-Plagiatssoftware.

Datum	Unterschrift